arXiv:cond-mat/0506178v1 [cond-mat.soft] 7 Jun 2005

Conformational transformations induced by the charge-curvature interaction

Yu. B. Gaididei
Bogolyubov Institute for Theoretical Physics, Metrologichna str. 14 B, 01413, Kiev, Ukraine

P. L. Christiansen
Informatics and Mathematical Modelling and Department of Physics,
The Technical University of Denmark, DK-2800 Lyngby, Denmark

W. J. Zakrzewski
Department of Mathematicccal Sciences, University of Durham,
Science Laboratories, South Road, Durham DH1 3LE, England

(Dated: February 2, 2008)

A simple phenomenological model for describing the conformational dynamics of biological macromolecules via the nonlinearity-induced instabilities is proposed. It is shown that the interaction between charges and bending degrees of freedom of closed molecular aggregates may act as drivers giving impetus to conformational dynamics of biopolymers. It is demonstrated that initially circular aggregates may undergo transformation to polygonal shapes and possible application to aggregates of bacteriochlorophyl *a* molecules is considered.

PACS numbers:

I. INTRODUCTION

The functioning of biological macromolecules is determined by their tertiary structure and different types of semiflexible polymers in solutions exhibit a variety of *conformational phase transitions* [1]. Even modest conformational changes modify long-range electronic interactions in oligopeptides [2], they may remove steric hindrances and open the pathways for molecular motions which are not available in rigid proteins [3]. In particular, it has been recently shown [4] that flexibility increases the hydrogen accessibility of DNA fragments and in this way facilitates strand breaks in DNA molecules. There is also a strong belief that the conductivity of DNA is due to thermal motion of small polarons [7, 8, 9].

Research in solitonic properties of the *chains with a bending* has been initiated in the recent years [5, 6, 10, 11, 12]. In particular, it was shown that the bending of the chain could manifest itself as an effective trap for nonlinear excitations [5, 10, 12] and that the energy of excitations decreases when the curvature of the bending increases [10].

Quite recently, there has been a growing interest in studying nonlinear charge and energy transport in soft condensed systems (polymers, membranes) with self-consistent account of coupling between nonlinear excitations and the shape of the systems. It has been demonstrated [18] that a mismatch of length scales in the presence of magnetic solitons leads to an elastic deformation on a soft magnetic surface. A phenomenological model for describing the conformational dynamics of biopolymers via the nonlinearity-induced buckling and collapse instability was proposed in [20]. It was shown there that the nonlinear excitations may cause local softening of polymer bonds. That is the effective bending rigidity of a chain may become negative nearby the nonlinear excitation and in this way the nonlinear excitation causes a buckling instability of the chain.

In this paper we study a simple model for electron-curvature interactions on closed molecular aggregates. In particular we show that due to the interaction between electrons and the bending degrees of freedom the circular shape of the aggregate may be become unstable and the aggregate takes the shape of an ellipse or a polygon. It is shown that the interaction between complexes may stabilize the ringlike shape of the The paper is organized as follows. The theory is applied to study the conformational transitions in light-harvesting complexes in purple bacteria. In Sec. II we describe a model. In Sec. III we present an analytical solution to the Euler-Lagrange equation. In Sec.III we compare our analytical results to results obtained directly by numerical simulations. In Sec. IV the interplay between shape of complexes and intercomplex interaction is studied. Sec. V is devoted to application to conformational transformations in light-harvesting complexes. Sec. VI presents some concluding remarks.

II. THE MODEL

Let us consider a chain consisting of L units labelled by an index n, and located at the points $\vec{r}_n = \{x_n,\, y_n,\, z_n\}$. We are interested in the case when the chain is closed and so we impose the periodicity condition on the coordinates $\vec{r}_n$

$$\vec{r}_n = \vec{r}_{n+L}. \tag{1}$$

The chain flexibility is accounted for by employing a microstructure consisting of many sequentially joined rigid rods and by incorporating a bend potential at each point of rotation [21]. Thus the Hamiltonian of such a polymer chain has the form

$$H = U + H_{el}, \tag{2}$$

with the potential energy of inter-unit interactions $U(...,\vec{r}_n,\vec{r}_{n+1},..)$ which we take in the form

$$U = U_S + U_B \tag{3}$$

where

$$U_s = \frac{\sigma}{2}\sum_n \left(|\vec{r}_n - \vec{r}_{n+1}| - a\right)^2 \tag{4}$$

is the stretching energy in the harmonic approximation. Here a is an equilibrium distance between units (in what follows we assume $a = 1$) and σ is a dimensionless elastic modulus of the stretching rigidity of the chain, and

$$U_b = \frac{k}{2}\sum_n \frac{\kappa_n^2}{1 - \kappa_n^2/\kappa_{max}^2} \tag{5}$$

is the bending energy. Furthermore,

$$\kappa_n \equiv |\vec{\tau}_n - \vec{\tau}_{n-1}| = 2\,\sin\frac{\alpha_n}{2} \tag{6}$$

determines the curvature of the chain at the point n. The vector

$$\vec{\tau}_n = \frac{\vec{r}_{n+1} - \vec{r}_n}{|\vec{r}_{n+1} - \vec{r}_n|} \tag{7}$$

is the unit tangent vector, α_n is the angle between the tangent vectors $\vec{\tau}_n$ and $\vec{\tau}_{n-1}$, $\kappa_{max} = 2\,\sin\left(\alpha_{max}/2\right)$ with α_{max} being the maximum bending angle, k is the elastic modulus of the bending rigidity of the chain.

We assume that there is a small amount of extra electrons (or holes) on the chain. The Hamiltonian of electrons and their interaction with conformational degrees of freedom is

$$H_{el} = H_{hop} + H_{el-conf}, \tag{8}$$

where

$$H_{hop} = J \sum_n \Big|\psi_n - \psi_{n+1}\Big|^2 \,, \tag{9}$$

describes the motion of electrons along the chain, and

$$H_{el-conf} = -\frac{1}{2} \sum_n \chi \, \left(|\psi_{n+1}|^2 + |\psi_{n-1}|^2\right) \, \kappa_n^2 \tag{10}$$

gives the interaction between electrons and bending degrees of freedom. In Eqs. (8)-(10) $\psi_n(t)$ is the electron wave function at the site n, the parameter J describes the electron hopping in the chain, and χ is the curvature-electron coupling constant (see Appendix for details).

The quantity

$$\nu \equiv \frac{1}{L} \sum_n |\psi_n|^2 \tag{11}$$

gives the total density of extra electrons which can move along the chain and participate in the formation of the conformational state of the system. We will neglect the interaction between electrons. It is legitimate when the total density of electrons in the chain ν is small. Combining Eqs. (5) and (10), we notice that the effective bending rigidity changes close the points where the electron is localised. For positive values of the coupling constant χ there is a local softening of the chain, while for χ negative there is a local hardening of the chain.

In what follows we assume that the chain is planar ($z_n = 0$) and inextensible ($\sigma \to \infty$):

$$|\vec{r}_n - \vec{r}_{n+1}| = 1. \tag{12}$$

III. CONTINUUM APPROACH

We are interested here in the case when the characteristic size of the excitation is much larger than the lattice spacing. This permits us to replace $\psi_n(t)$ by the function $\psi(s,t)$ of the arclength s which is the continuum analogue of n. Using the Euler-Mclaurin summation formula [22] we get

$$H = U_b + H_{el}, \tag{13}$$

$$U_b = \frac{1}{2} k \int_0^L \kappa(s)^2 \, ds \tag{14}$$

$$H_{el} = \int_0^L \left\{ J \Big|\partial_s \psi\Big|^2 - \chi \, \kappa(s)^2 \, |\psi|^2 \right\} ds. \tag{15}$$

Being interested here in small curvature effects: $\kappa(s) \ll \kappa_{max}$, we consider the bending energy in the harmonic approximation given by Eq. (14).

A. Ground state of the chain

The electron ground state wave function $\phi(s)$ and the shape of the chain $\vec{r}(s)$ may be obtained by minimizing the functional

$$\mathcal{E} = H_{el} + U_b \tag{16}$$

with H_{el} and U_b given by Eqs (15) and (14) under the constraint

$$\nu = \frac{1}{L}\int\limits_0^L \phi(s)^2\, ds, \tag{17}$$

which is a continuum analog of Eq. (11). The inextensibility constraint (12) reads in the continuum limit

$$|\partial_s \vec{r}|^2 = 1. \tag{18}$$

The inextensibility constraint (18) is automatically taken into account by choosing the parametrization

$$\partial_s\, x(s) = \sin\theta(s), \quad \partial_s\, y(s) = \cos\theta(s) \tag{19}$$

where the angle $\theta(s)$ satisfies the conditions

$$\theta(s+L) = 2\pi + \theta(s) \tag{20}$$

and

$$\int\limits_0^L \cos\,\theta(s)\, ds = \int\limits_0^L \sin\,\theta(s)\, ds = 0 \tag{21}$$

which follow from Eq. (1). Note that, in the continuum limit, the curvature of the chain $\kappa(s)$ given by Eq. (6) can be expressed as

$$\kappa(s) = |\partial_s^2 \vec{r}(s)|. \tag{22}$$

Thus, in the frame of the parametrization (19), $\kappa(s) = \partial_s\theta$ and the functional (16) takes the form

$$\mathcal{E} = \int\limits_0^L \left\{ J\,\nu\,\left(\partial_s\varphi\right)^2 + \left(\frac{k}{2} - \chi\,\nu\,\varphi^2\right)\,\left(\partial_s\theta\right)^2 \right\} ds, \tag{23}$$

where the rescaled function $\varphi(s) = \sqrt{\nu}\,\phi(s)$ which satisfies the normalization condition

$$\frac{1}{L}\int\limits_0^L \varphi^2(s) = 1, \tag{24}$$

has been introduced.

The Euler-Lagrange equations for the problem of minimizing $\mathcal{E}$, given by Eq. (23) under the constraint (24) become

$$\partial_s^2\varphi + \frac{\chi}{J}\,\left(\partial_s\theta\right)^2\,\phi - \lambda\varphi = 0, \tag{25}$$

$$\partial_s\left(\partial_s\theta\,\left(1 - w\,\varphi^2\right)\right) = 0 \tag{26}$$

where λ is the Lagrange multiplier and

$$w = \frac{2\,\chi\,\nu}{k} \tag{27}$$

is a coupling constant which characterizes the strength of the charge-curvature interaction in terms of the bending rigidity of the chain and the charge density. We are interested in solutions of Eq. (25) subject to the periodic boundary conditions

$$\varphi(s) = \varphi(s + \frac{L}{n}). \tag{28}$$

where n is an integer which characterizes the shape of the chain (see below). Integrating Eq. (26), we get

$$\partial_s \theta = \frac{A}{1 - w\,\varphi^2} \tag{29}$$

where A is an integration constant. Taking into account the condition (20) we obtain that the integration constant A is determined by the relation

$$A = \frac{2\pi}{L}\, I \tag{30}$$

where the functional I is given by the relation

$$\frac{1}{I} = \frac{1}{L}\int\limits_0^L \frac{ds}{1 - w\,\varphi^2}. \tag{31}$$

From Eqs. (19) and (29) we see that the shape of the chain is determined by the equations

$$x(s) = \int\limits_0^s sin\,\theta(s')\,ds', \quad y(s) = \int\limits_0^s cos\,\theta(s')\,ds',$$

$$\theta(s) = \frac{2\pi}{L\,I}\int\limits_0^s \frac{1}{1 - w\,\varphi^2(s')}\,ds'. \tag{32}$$

B. Solution of the Euler-Lagrange equations

There are two kinds of solutions to Eqs (25) and (29).

- Circular chain.
  Charge is uniformly distributed along the chain

  $$\varphi = 1 \tag{33}$$

  where the normalization condition (17) has been used, and the curvature of the chain is constant

  $$\kappa(s) \equiv \partial_s \theta = \frac{A}{1 - w}. \tag{34}$$

  This case corresponds to a circular chain

  $$x = R\,\sin\frac{s}{R}, \quad y = -R\cos\frac{s}{R}.$$

  The radius R of the circle can be obtained by puting Eq. (34) into the boundary condition (20). As a result we have

  $$R = \frac{L}{2\pi}. \tag{35}$$

  The energy of the circular chain is thus

  $$\mathcal{E}_{circ} = \frac{2\pi^2}{L}\,k(1 - w). \tag{36}$$

- Polygonally deformed chain.

Let us consider now the case of spatially non-uniform distributed electrons. Inserting Eqs. (29)-(31) into Eq. (23) we get

$$\mathcal{E} = J\,\nu \int\limits_0^L (\partial_s \varphi)^2 \; ds + \frac{2\pi^2 k}{L}\, I. \tag{37}$$

We restrict our analytical consideration to the case when the charge-curvature coupling is weak and/or the charge density is low: $w \ll 1$. Expanding the functional I in terms of the small parameter w we obtain from Eq. (37)

$$\mathcal{E} = \frac{2\pi^2\, k}{L\,(1+w)} + J\,\nu \int\limits_0^L \Big\{ (\partial_s \varphi)^2 - \frac{G\nu}{R^2}\, \varphi^4 - w\, \frac{G\nu}{R^2}\, \varphi^6 \Big\}\, ds \tag{38}$$

where

$$G = \frac{2\chi^2}{J\, k\, (1+w)^2} \tag{39}$$

is an effective nonlinear parameter. For small w one can neglect the last term in Eq. (38) and the Euler-Lagrange equation for the functional (38) then takes the form

$$\partial_s^2 \varphi + 2 \frac{G\,\nu}{R^2}\, \varphi^3 - \lambda\, \varphi = 0. \tag{40}$$

Straightforward calculations show that Eq. (40) has a solution of the form

$$\varphi = R \sqrt{\frac{\lambda}{(2-m)\, G\, \nu}}\, dn \left(\sqrt{\frac{\lambda}{(2-m)}}\; s \Big| m \right) \tag{41}$$

where $dn(u|m)$ is the Jacobi elliptic function with the modulus m [22]. Inserting Eq. (41) into the boundary condition (28) and the normalization condition (24), we find that the Lagrange multiplier λ and the modulus m are determined by the equations

$$\sqrt{\frac{\lambda}{(2-m)}}\, \frac{L}{n} = 2\, K(m) \tag{42}$$

$$G\,\nu = \frac{n^2}{\pi^2}\, K(m) E(m) \tag{43}$$

and the charge distribution along the chain is given by

$$\varphi = \sqrt{\frac{K}{E}}\, dn \left(\frac{2\, n\, K}{L}\; s \Big| m \right) \tag{44}$$

where $K(m)$ and $E(m)$ are the complete elliptic integrals of the first kind and the second kind, respectively [22]. The curvature of the chain is given by the equation

$$\kappa(s) \equiv \partial_s \theta \approx \frac{1}{R}\, I \left(1 + w\, \frac{K}{E}\, dn^2 \left(\frac{2n\, s\, K}{L} \Big| m \right) \right). \tag{45}$$

Integrating Eq. (45), we get

$$\theta(s) = \frac{2\pi}{L}\, I \left(s + w\, \frac{L}{2\, n\, E}\, E\left(\alpha | m \right) \right) \tag{46}$$

where $E\left(\alpha\middle|m\right)$ is the incomplete elliptic integral of the second kind, and $\alpha = am\left(\frac{2\,n\,K}{L}\,s\middle|m\right)$ is the amplitude function [22]. By using the Fourier expansion for the amplitude function for small m we obtain from Eq. (46)

$$\theta(s) \approx \frac{2\pi}{L}\,(1+w)\,I\,s + \frac{w}{4n}\,I\,m\,\sin\left(\frac{2n\pi}{L}\,s\right). \tag{47}$$

Inserting Eq. (47) into the closure condition (21), we find that it is satisfied for $n \geq 2$. Eqs. (32) and (47) describe a polygon: for $n = 2$ it is an elliptically deformed chain, while for $n = 3$ it has a triangular shape (see Fig. 1). We see from Eqs. (44) and (45) that the polygon structure is a result of the self-consistent interaction between electrons and bending degrees of freedom: extrema of the curvature and of the charge density correlate: in the case of the softening electron-curvature interaction ($\chi > 0$ maxima of curvature and charge density coincide, while in the case of the hardening interaction the minima of the curvature coincide with the maxima of the charge density. Eq. (43) shows that, for a given value of the nonlinear parameter G, the n-gon structure appears when the charge density exceeds the threshold value ν_n:

$$\nu\, > \nu_n \equiv \frac{n^2}{4\,G} \tag{48}$$

.

The energy difference between the n-gon structure and the circular chain is given by the expression

$$\mathcal{E}_n - \mathcal{E}_{circ} = \frac{4\pi^2}{3\,L}\,\frac{G\,J\,\nu^2}{E^2}\,\left(3E^2 - (2-m)EK - (1-m)K^2\right). \tag{49}$$

The normalized energy difference

$$\Delta_n = \frac{\mathcal{E}_n - \mathcal{E}_{circ}}{\mathcal{E}_{circ}} \tag{50}$$

for $n = 2, 3$ versus the charge density is shown in Fig. 2. We note that when the charge density is above the critical value the deformed structure with spatially inhomogeneous charge distribution is energetically more favorable than the circular system with a uniformly distributed charge. The state with elliptically deformed chain $n = 2$ is the energetically most preferable.

Note also that our analytical approach was based on the assumption that $w\,\varphi^2 \ll 1$. Taking into account Eq. (44), this means that it is legitimate to consider not too sharp distributions which correspond to $w\,K(m) \ll 1$ or $m \ll 1 - \exp\{-0.72/w\}$.

IV. NUMERICAL STUDIES

To check our results we have performed also several numerical studies. To this end we carried out the dynamical simulations of the equations

$$\eta\frac{d}{dt}\vec{r}_n = -\frac{\partial H}{\partial\,\vec{r}_n}, \tag{51}$$

$$i\,\frac{d}{dt}\psi_n = -\frac{\partial\,H}{\partial\,\psi_n^*} \tag{52}$$

with the Hamiltonian H being defined by Eqs. (2)-(10). Thus the conformational dynamics is considered in an overdamped regime with the friction coefficient η. Then we took as our starting configurations systems involving the electric charge density of (almost) the same magnitude (ψ_n) at all points (we broke the symmetry by increasing the density at one point of the chain by 1%). Initially, all the lattice points were placed at symmmetric points on the circle of an appropriate radius (see Fig.3). We performed such simulations for several values of the charge density. Due to the absorption the energy of the system was decreasing during the evolution and the system was evolving towards a minimum. At the same the points of the chain were moving from their initial to their new positions.

We considered both the cases of the hardening and of the softening electron-curvature interaction.

In the case of a hardening electron-curvature interaction ($\chi < 0$) a typical final distribution of the chain points is shown in Fig.4. The charge density and the curvature distributions are in full agreement with the results of our analytical considerations: the curve is more flat where the density of the electrons is maximal. In fact, the ellipse-like shape is rather robust as it arises for a large range of parameters (of the strength of the hardening electron-curvature interaction and of the anharmonicity coefficient κ_{max}).

Complexes with a softening electron-curvature interaction are much more flexible. Their equilibrium shape depends drastically both on the anharmonicity and on the charge density. Figs 5 and 6 demonstrate how drastically the shape of the complex and the charge distribution along the chain can change as a function of the total charge density ν: increasing the total charge by 5% can lead to the localisation of almost the whole charge of the system at one place.

In our numerical work we also studied the stability of our 'final' field configurations - i.e. the configurations which we thought the system was settling at. This we studied by perturbing the system. Such perturbations were introduced in two stages. First we changed the electric charge of the configuration by multiplying all 'final' values of the electric charge by a constant factor μ; this had the effect of changing the energy of the system. Then we performed the new minimisation and, when the system appeared to have settled at the new 'final' configuration, we changed back its ψ_n by a new multiplication by $1/\mu$. As $\sum_n |\psi_n|^2$ is conserved during the evolution, the final system had the same value of it as the original 'unperturbed' fields. The results of the further minimisation were then compared with the original 'final' fields.

When we applied this technique to our field configuration shown in Fig. 6 we found that the system was really unchanged by this perturbation; in fact the perturbation led to an overall rotation of the system by one lattice point, but the sequence of values of the fields was essentially the same thus showing the stability of the found minimum.

V. EFFECTS OF INTERCOMPLEX INTERACTION

The aim of this section is to investigate how the interaction between complexes influences the shape. We will consider the system which is described by the Hamiltonian

$$\mathcal{H} = \sum_j \mathcal{E}_j + \frac{1}{2}\sum_{i,j} U_{i\,j}, \tag{53}$$

where $\mathcal{E}_j$ is the energy of the j-th aggregate which is given by Eq. (23) with φ replaced by φ_j and θ replaced by θ_j, and U_{ij} is the interaction energy between particles. The latter we will take in the form of the Gay-Berne potential [25] which is a generalization of the Lennard-Jones 12-6 potential and is widely used to study translational and orientational ordering in systems of aspherical molecules. We consider small deviations from the ringlike structure of aggregates and so we neglect the difference of the well depths for side-to-side and end-to-end configurations. In this case the Gay-Berne potential between two parallel uniaxial molecules is given by

$$U_{ij} \equiv U\left(\vec{r}_{ij}\right) = \frac{U_0}{\sqrt{1-\zeta^2}}\Big[\left(\frac{\sigma_0}{r_{ij} + \sigma\left(\hat{\vec{r}}_{ij}\right) + \sigma_0}\right)^{12} - \left(\frac{\sigma_0}{r_{ij} + \sigma\left(\hat{\vec{r}}_{ij}\right) + \sigma_0}\right)^{6}\Big] \tag{54}$$

where $\vec{r}_{ij} = r_{ij}\hat{\vec{r}}_{ij}$ is the interparticle vector,

$$\sigma\left(\hat{\vec{r}}_{ij}\right) = \sigma_0\left[1 - \frac{2\zeta}{1+\zeta}\left(\hat{\vec{r}}_{ij}\cdot\vec{e}\right)^2\right]^{-1/2} \tag{55}$$

is the anisotropy parameter where $\vec{e}$ is a unit vector specifying the axes of symmetry. The anisotropy coefficient ζ is determined by the lengths of the major and minor axes $\sigma_{||}$ and $\sigma_{\perp}$

$$\zeta = \frac{\sigma_{||}^2 - \sigma_{\perp}^2}{\sigma_{||}^2 + \sigma_{\perp}^2} \tag{56}$$

and σ_0 gives a charasteristic length scale while U_0 determines the intensity of the interaction.

The centers of densely packed circular aggregates of the radius R create a two-dimensional triangular lattice $\vec{r}_j = j_1\vec{a}_1 + j_2\vec{a}_2, \quad (j \equiv (j_1, j_2),\ j_1, j_2 = 0, \pm1, \pm2, ...)$ with the basic vectors $\vec{a}_1 = \ell\,(1, 0)$ and $\vec{a}_2 = \ell\,\left(1/2, \sqrt{3}/2\right)$ where ℓ is the lattice constant (see Fig. 7). Being elliptically deformed in such a way that the major axes of all aggregates are parallel to the x-axis, the centres of densely packed elliptical aggregates create a lattice $\vec{r}_j = j_1\vec{b}_1 + j_2\vec{b}_2$ with the basic vectors $\vec{b}_1 = \ell\,(1+u, 0)$ and $\vec{b}_2 = \ell\,\left(1/2\,(1+u), \sqrt{3}/2\,(1-u)\right)$ (see Fig. 8), where the parameter u is given by

$$u = \frac{\sigma_{||} - \sigma_{\perp}}{\sigma_{||} + \sigma_{\perp}}. \tag{57}$$

Now we study the ground state of this system by using a trial function approach. We assume that this state is spatially homogeneous and relying on the results of the previous section, we assume that the electron trial function and the trial curvature can be taken in the form

$$\varphi_j = \left(\cos\alpha + \sqrt{2}\,\sin\alpha\,\cos\left(\frac{2\,s}{R}\right)\right), \tag{58}$$

$$\partial_s\,\theta_j = \frac{1}{R}\left(1 + \gamma\,\cos\left(\frac{2\,s}{R}\right)\right) \tag{59}$$

The functions (58) and (59) can be considered as a truncated Fourier expansion of the solutions (41) and (45) in which the coefficients α and γ are variational parameters and R is the radius of the cylindrically symmetric aggregate. The function (58) satisfies both the periodicity condition (28) and the number of particles constraint (17). In the limit $\gamma < 1$ the shape of the curve with the curvature given by Eq. (59) is parametrically determined by the expressions

$$\begin{aligned} x(s) &= R\left((1+\frac{\gamma}{4})\,\cos\left(\frac{s}{R}\right) + \frac{\gamma}{12}\,\cos\left(\frac{3\,s}{R}\right)\right), \\ y(s) &= R\left((1-\frac{\gamma}{4})\,\sin\left(\frac{s}{R}\right) + \frac{\gamma}{12}\,\sin\left(\frac{3\,s}{R}\right)\right). \end{aligned} \tag{60}$$

Thus the lengths of the major and minor axes of the curve (60) are given by

$$\sigma_{||} = R\,(1+\frac{\gamma}{3}), \qquad \sigma_{\perp} = R\,(1-\frac{\gamma}{3}) \tag{61}$$

and comparing Eqs (57) and (61), we see that $u = \gamma/3$.

Inserting Eqs. (58) and (59) into Eqs. (53), (23) and (54) for an energy per aggregate we get

$$\frac{\mathcal{H}}{N_a} = \mathcal{E}_{tr} + U \tag{62}$$

where

$$\mathcal{E}_{tr} = \frac{\pi\,k}{R}\left\{1 + \frac{\gamma^2}{2} - \frac{1}{8}\,\xi\nu\,\left(8 + 5\gamma^2 - \gamma^2\,\cos(2\,\alpha) + 8\sqrt{2}\,\sin(2\,\alpha)\right) + \frac{4\,J}{k}\,\nu\,\sin^2\alpha\right\} \tag{63}$$

is the energy of an isolated aggregate, and

$$U = \sum_{j=0}^{5} U\left(\vec{\Delta}_j\right) \tag{64}$$

is the energy due to the interaction between aggregates in the lattice. In Eq. (64) the function $U\left(\vec{\Delta}_j\right)$ is given by Eqs. (54), (55) with $\vec{e} = (1,\ 0)$ and vectors $\vec{\Delta}_j = \sigma_0\ \left((1+\frac{\gamma}{3})\ \cos\left(\frac{\pi j}{3}\right), (1-\frac{\gamma}{3})\ \sin\left(\frac{\pi j}{3}\right)\right)$ connect nearest and next-nearest neighbours of the lattice. The interaction energy (64) has a minimum at $\ell = 2^{1/6}\,\sigma_0, \quad \gamma = 0$ which corresponds to a system of densely packed circular aggregates. Expanding the function (64) in the vicinity of this point, in powers of the variational parameter γ, we get

$$U = -\frac{3}{2}\,U_0 + c\,U_0\,\gamma^2 + \cdots \tag{65}$$

where the numerical coefficient $c \approx 2.05$. According to the variational principle we should satisfy the equations

$$\partial_\alpha\,\mathcal{E}_{tr} = 0, \tag{66}$$

$$\partial_\gamma\,\left(\mathcal{E}_{tr} + U\right) = 0. \tag{67}$$

From Eq. (66) we get

$$\tan(2\alpha) = \frac{8\sqrt{2}k\,\xi}{32\,J - k\,\xi\,\gamma^2}\,\gamma. \tag{68}$$

Inserting Eq. (68) into Eq. (63) and expanding it in terms of γ we obtain that

$$\mathcal{E}_{tr} = \mathcal{E}_{circ} + \frac{\pi\,k}{2\,R}\left(1 - \frac{\nu}{\nu_{cr}}\right)\gamma^2 + B\,\gamma^4 + \cdots \tag{69}$$

where

$$\nu_{cr} = \frac{k}{2\,\chi}\,\frac{J}{J+\chi} \tag{70}$$

is the critical charge density and the notation

$$B = \frac{\pi}{16\,R}\frac{\chi^3\,\nu}{J^3}\,(2\chi - J)$$

is introduced. Thus in the framework of the variational approach the energy of a single complex has a single minimum at $\gamma = 0$ when $\nu\ <\ \nu_{cr}$ and in this case the aggregate has a ring-like shape. When $\nu\ >\ \nu_{cr}$ and $2\,\chi > J$ the energy (69) possesses two equivalent minima with $\pm\gamma_0$ $(\gamma_0 \neq 0)$ (see Fig. 9). As it is seen from Eqs. (60) the finite value of γ_0 implies that the aggregate is elliptically deformed either along the x-axis (when $\gamma > 0$) or along the y-axis (when $\gamma < 0$). Note that in the limit $\chi \gg J$, ν_{cr} coincides with ν_2 given by Eq. (48). Combining (65) and (69) we see that the interaction between aggregates modifies the condition for appearance of the low-symmetry form. Indeed, even in the case when $\nu > \nu_{cr}$ (an isolated aggregate has an ellipse-like shape) in the condensed phase of aggregates for strong enough inter-aggregate interaction we may have an inequality

$$\nu\ <\ \nu_{cr}\,\left(1 + \frac{2\,c\,U_0}{\pi\,k}\,R\right) \tag{71}$$

which means that interacting aggregates are ring-like and create a densely packed crystallic structure with the group symmetry D_{6h} (see Fig. 7).When

$$\nu\ >\ \nu_{cr}\,\left(1 + \frac{2\,c\,U_0}{\pi\,k}\,R\right) \tag{72}$$

the ellipse-like shape survives in the condensed phase which has a rectangular unit cell and transforms in accordance with the group symmetry D_{2h} (see Fig.8). There are two equivalent types of arrangement in the low-symmetry phase when the aggregates are elliptically deformed either along the x-axis (when $\gamma > 0$) or along the y-axis (when $\gamma < 0$). In accordance with this the condensed phase of the aggregates must have a domain structure, *i.e.* it must consist of various regions in which the direction of long axes are different.

VI. APPLICATION TO BACTERIOCHLOROPHYLL *a* COMPLEXES

The X-ray crystallography shows [23] that bacteriochlorophyll a (Bchl a) molecules in the LH complex are organized in two concentric rings: the B800 and B850 rings. The former consists of nine well-separated Bchl a molecules with an absorption band at 800 nm and the latter consists of 18 Bchl molecules with an absorption band at 860 nm (see Fig. 1 in Ref. [15]). Measurements of the anisotropic properties of the absorption of isolated LH2 complexes from bound to mica surfaces [13], the fluorescence-excitation spectra of individual LH2 complexes from bacteria *Rhodopseudomonas acidophila* [14, 15, 16] showed that the complexes are generally not cylindrically symmetric but reveal a deformation of the circular complex into a shape with C_2 symmetry. Quite recently the shape of the LH2 complex from bacteria *Rhodobacter spheroides 2.4.1* in detergent solution has been determined from synchrotron small-angle X-ray scattering data [17]. It was shown that, in contrast to the cylindrical crystal structure with a diameter of $6.8nm$, the shape of an isolated LH2 complex is an oblate plate with an eccentricity $\epsilon = 0.59$. It was conjectured in Ref. [14] that the extremely dense packing of LH2 in the crystals causes the cylindrical symmetry of the complexes. A variety in shapes and conformations for light-harvesting LH1 complexes and different types of their packing in two-dimensional crystals revealed by atomic force microscopy were reported recently in Ref. [24].

A qualitative explanation of this phenomena follows from the theory developed in previous sections. It has shown that in the presence of sufficiently strong charge-curvature interaction an isolated complex has an ellipse-like shape while the interaction between complexes in the form of an anisotropic Gay-Berne potential stabilizes the ringlike shapes of the complexes. However if the intensity of the intercomplex interaction is less than some threshold value (see Eqs. (65) and (69)) the non-circular shape of the complex is preserved in the condensed phase.

The model is too simplified for quantitative predictions for light-harvesting complexes but we believe that it contains interesting physics which should be important for further studies of such systems.

VII. CONCLUSIONS

In this paper, we have investigated the role of the electron-curvature interaction on the formation of the ground state of closed semiflexible molecular chains. We have found that the coupling between electrons and the bending degrees of freedom of the chain can induce a local softening or hardening of chain bonds, *i.e.* the effective bending rigidity of the semiflexible chain changes as the density of charge changes along the chain. When the charge density and/or the strength of the electron-curvature coupling exceed a threshold value, the spatially uniform distribution of the charge along the chain and the circular, cylindrically symmetric shape of the chain become unstable. In this case the ground state of the system is characterized by a spatially non-uniform distribution of electrons along the chain and the chain takes on an ellipse-like (or in general polygon-like) form.

Acknowledgments

Yu. B. G. would like to thank L. Valkunas for attracting his attention to the problem of structural deformations of light-harvesting complexes. Yu.B.G. and W.J.Z. thank L. Brizhik, A. Eremko and B. Piette for their interest and helpful discussions. Yu.B.G. thanks for a Guest Professorship funded by Civilingeniør Frederik Christiansens Almennyttige Fond and MIDIT, SNF grant # 21-02-0500 as well as support from the research center of quantum medicine "Vidguk". He also thanks Department of Physics, the Technical University of Denmark for hospitality.

APPENDIX A

The electron-conformation interaction can be obtained from the Coulomb interaction between an electron and charged groups of the molecule

$$H_{int} = \sum_{n,n'} V\left(|\vec{r}_n - \vec{r}_{n'}|\right)\, |\psi_n|^2 \tag{A1}$$

where the matrix element $V\left(|\vec{r}_n - \vec{r}_{n'}|\right)$ describes the Coulomb interaction between an electron which occupies the site n in the chain and the charged group at the site n'. From the inextensibility condition (12) we see that the nearest neighbour interaction terms ($|n-n'|=1$) do not contribute to the electron-conformational interaction. Taking into account that

$$\left(\vec{r}_{n+2} - \vec{r}_n\right)^2 = 2a^2 + 2\,\left(\vec{r}_{n+1} - \vec{r}_n\right)\cdot\left(\vec{r}_{n+2} - \vec{r}_{n+1}\right) = 4a^2 - a^2\kappa_{n+1}^2 \tag{A2}$$

we obtain from Eq. (A1) that, in the next-nearest-neighbour approximation, the energy of the electron-conformational interaction takes the form

$$H_{el-conf-app} = -\frac{1}{2}\sum_n \chi\,\left(\kappa_{n+1}^2 + \kappa_{n-1}^2\right)\,|\psi_n|^2 \tag{A3}$$

where the notation

$$\chi = \frac{1}{2}\, a\, \frac{dV}{dr}\Big|_{r=2a} \tag{A4}$$

has been used.

---

[1] A. L. Kholodenko and T. A. Vilgis, Phys. Rep. **298**, 254 (1998).

[2] J. Wolfgagng, S.M. Risser, S. Priyardshy, and D.N. Beratan, J. Phys. Chem **101**, 2986 (1997).

[3] J. Feitelson and G. McLendon, Biochemistry, **30**, 5051 (1991).

[4] D. Viduna, K. Hinsen and G. Kneller, Phys. Rev. E **62**, 3986 (2000).

[5] J. J.-L. Ting and M. Peyrard, Phys. Rev. E **53**, 1011 (1996); K. Forinash, T. Cretegny, and M. Peyrard, Phys. Rev. E **55**, 4740 (1997).

[6] T. B. Polyakova and R. A. Suris, Solid State Commun. **77**, 825 (1991).

[7] E. M. Conwell and S.V. Rakhmanova, Proc. Natl. Acad. Sci. U.S.A. **97**, 4557 (2000).

[8] K.H. Yoo *et.al* Phys. Rev. Lett. **87**, 198102 (2001).

[9] S.S. Alexandre *et.al* Phys. Rev. Lett. **91**, 108105 (2003).

[10] Yu. B. Gaididei, S. F. Mingaleev, and P. L. Christiansen, Phys. Rev. E **62**, R53 (2000); P. L. Christiansen, Yu. B. Gaididei, and S. F. Mingaleev, J. Phys.: Condens. Matter, **13**, 1181 (2001).

[11] J. F. R. Archilla, P. L. Christiansen, S. F. Mingaleev, and Yu. B. Gaididei, J. Phys. A.: Math. Gen. **34**, 6363 (2001); J. Cuevas, J.F.R. Archilla, Yu.B. Gaididei and F.R. Romero, Physica D **163**, 106 (2002); J. F. R. Archilla, P. L. Christiansen, and Yu. B. Gaididei, Phys. Rev. E **65**, 016609 (2002).

[12] R. Reigada, J.M. Sancho, M. Ibanes, and G.P. Tsironis, J. Phys. A, **34**, 8465 (2001); M. Ibanes, J.M. Sancho, and G.P. Tsironis, Phys. Rev. E **65**, 041902 (2002).

[13] M. Bopp, A. Sytnik, T. D. Howard, R. J. Cogdell and R. M. Hochstrasser, Proc. Natl. Acad. Sci. USA, **96**, 11271 (1999).

[14] A. M. van Oijen, M. Ketelaars, J. Köhler, T. J. Aartsma, J. Schmidt, Science,**285**, 400 (1999).

[15] M. Ketelaars, A. M. van Oijen, M. Matsushita , J. Köhler, J. Schmidt, and T. J. Aartsma, Biophysical J. **80**, 1591 (2001).

[16] M. Matsushita, M. Ketelaars, A. M. van Oijen, , J. Köhler, T. J. Aartsma, and J. Schmidt, Biophysical J. **80**, 1604 (2001).

[17] X. Hong, Yu-X. Weng, and M. Li, Biophysical J. **86**, 1082 (2004).

[18] A. Saxena, R. Dandoloff, T. Lookman, Physica A **261**, 13 (1998).

[19] Y. Jiang, T. Lookman, and A. Saxena, Phys. Rev. E **61**, R57 (2000).

[20] S.F. Mingaleev, Yu. B. Gaididei, P.L. Christiansen, Yu. S. Kivshar, Europhys. Letters, **59**, 403 (2002).

[21] C. V. Chaubal, L. G. Leal, J. Polym. Science B, **37**,281 (1999).

[22] M. Abramowitz and I. Stegun, *Handbook of Mathematical Functions* (Dover Publications, Inc., New York, 1972).

[23] G. McDermott *et al. Nature*, **374** 517 (1995).

[24] S. Bahatyrova *et al.* J. Biol. Chemistry, **279**, 21327 (2004).

[25] J.G. Gay and B.J. Berne, J. Chem. Phys. **74**, 3316 (1981).

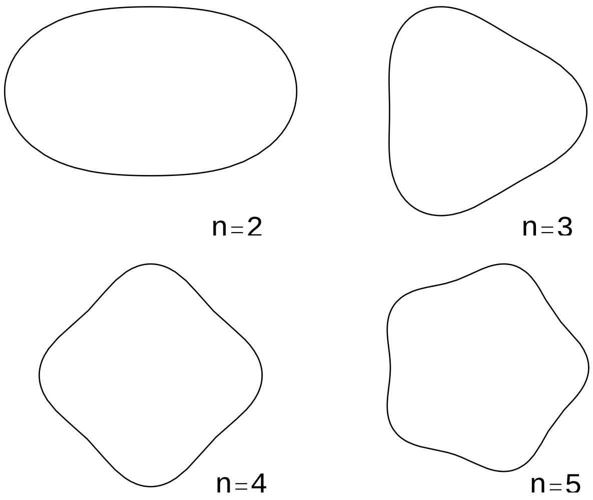

FIG. 1: The shape of the chain: in the ellipse-like state ($n = 2$), in the polygon states ($n = 3, 4, 5$).

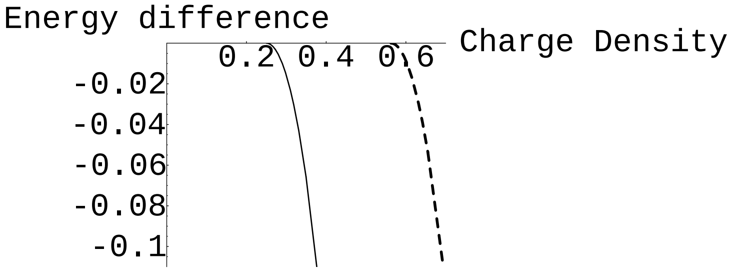

FIG. 2: The normalized energy difference Δ_n from Eq. (50 for the ellipse-like $n = 2$ (solid line) and triagon-like chain $n = 3$ (dashed line) with $2\chi = 4\,J = k$.

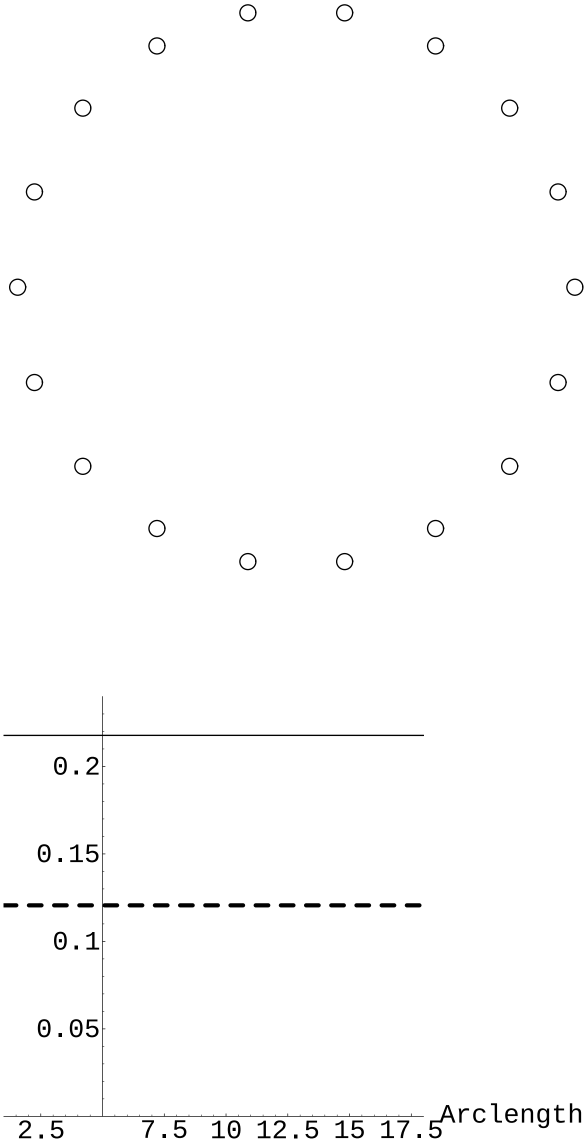

FIG. 3: The top panel shows the initial shape of the chain; the bottom panel shows the initial charge (solid line) and curvature (dashed line) distribution along the chain.

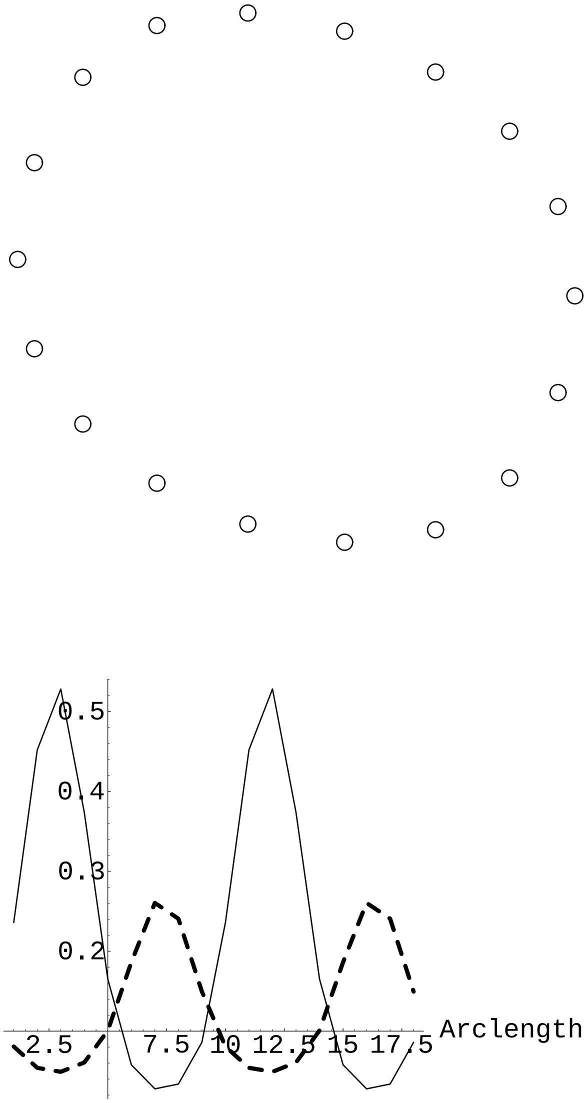

FIG. 4: The top panel shows the equilibrium shape of the chain, and the bottom panel shows the charge distribution (solid line) and curvature variation (dashed line) along the chain in the case of hardening electron-curvature interaction with $\nu = 0.22,\ \chi = -2,\ k = 1\ J = 0.4$

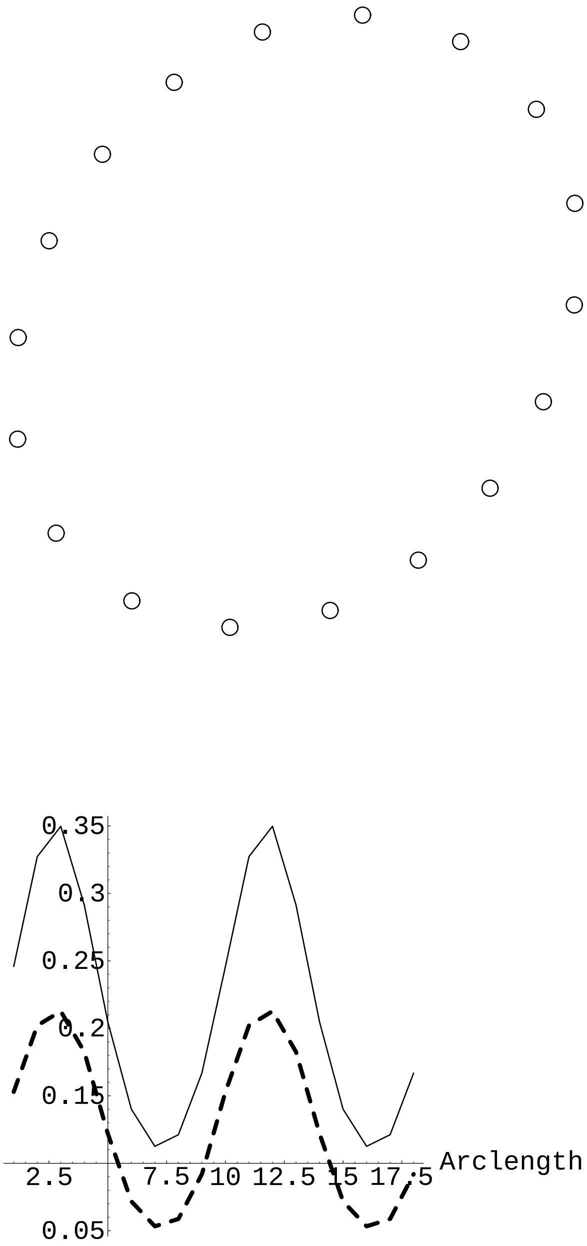

FIG. 5: The top panel shows the equilibrium shape of the chain and the bottom panel shows the charge distribution (solid line) and curvature variation (dashed line) along the chain in the case of softening electron-curvature interaction with $\nu = 0.22$, $\chi = 2.15$, $k = J = 1$

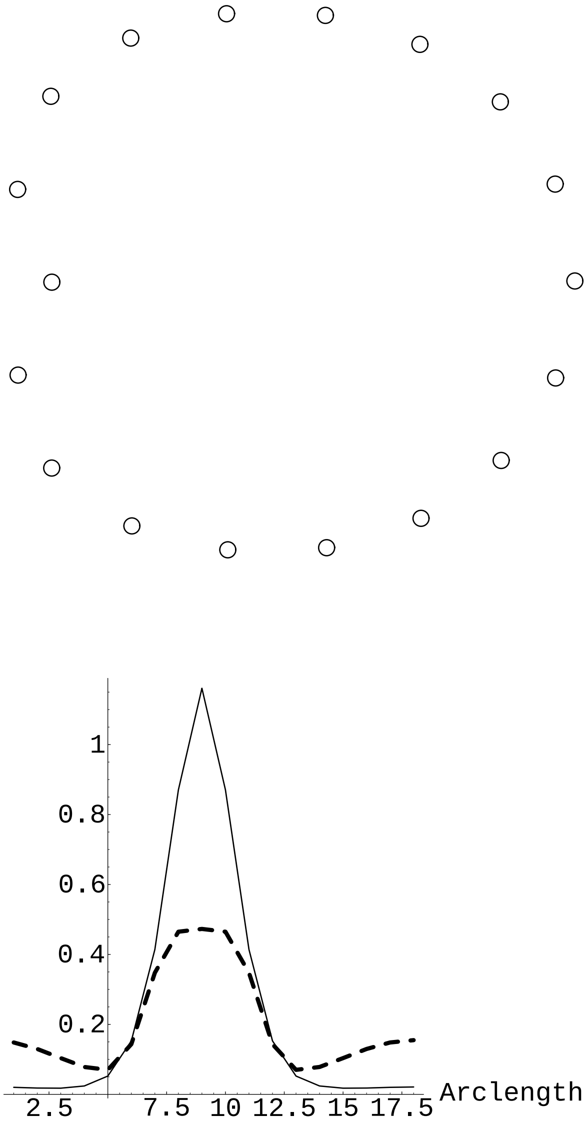

FIG. 6: Same as Fig. 5 with $\nu = 0.23$, $\chi = 2.15$, $k = J = 1$

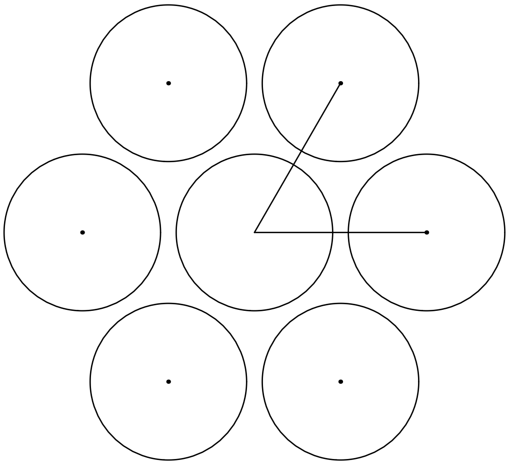

FIG. 7: Arrangement of densely packed ring-like aggregates.

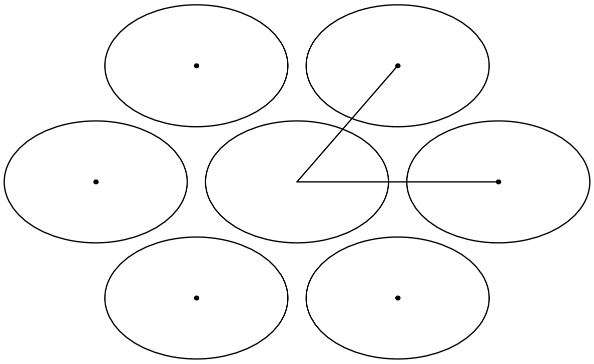

FIG. 8: Arrangement of densely packed ellipse-like aggregates.

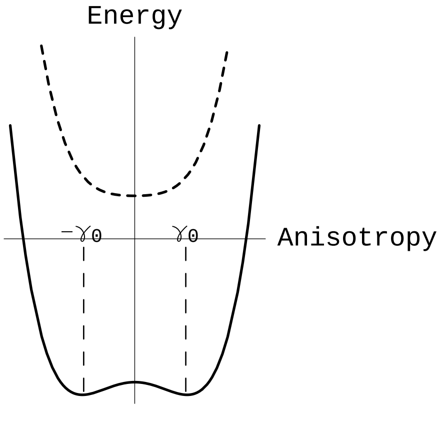

FIG. 9: Energy per aggregate (Eq. (62)) as a function of the trial anisotropy parameter γ for the charge density below the threshold (dashed) and above the threshold (solid).